Accepted Manuscript

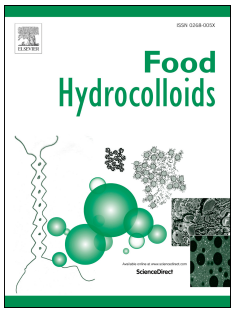

Unravelling the structure of serum pectin originating from thermally and mechanically processed carrot-based suspensions

Jihan Santanina J. Santiago, Clare Kyomugasho, Shashikant Maheshwari, Zahra Jamsazzadeh Kermani, Davy Van de Walle, Ann M. Van Loey, Koen Dewettinck, Marc E. Hendrickx

PII: S0268-005X(17)30334-X

DOI: 10.1016/j.foodhyd.2017.10.026

Reference: FOOHYD 4113

To appear in: *Food Hydrocolloids*

Please cite this article as: Jihan Santanina J. Santiago, Clare Kyomugasho, Shashikant Maheshwari, Zahra Jamsazzadeh Kermani, Davy Van de Walle, Ann M. Van Loey, Koen Dewettinck, Marc E. Hendrickx, Unravelling the structure of serum pectin originating from thermally and mechanically processed carrot-based suspensions , *Food Hydrocolloids* (2017), doi: 10.1016/j.foodhyd.2017.10.026

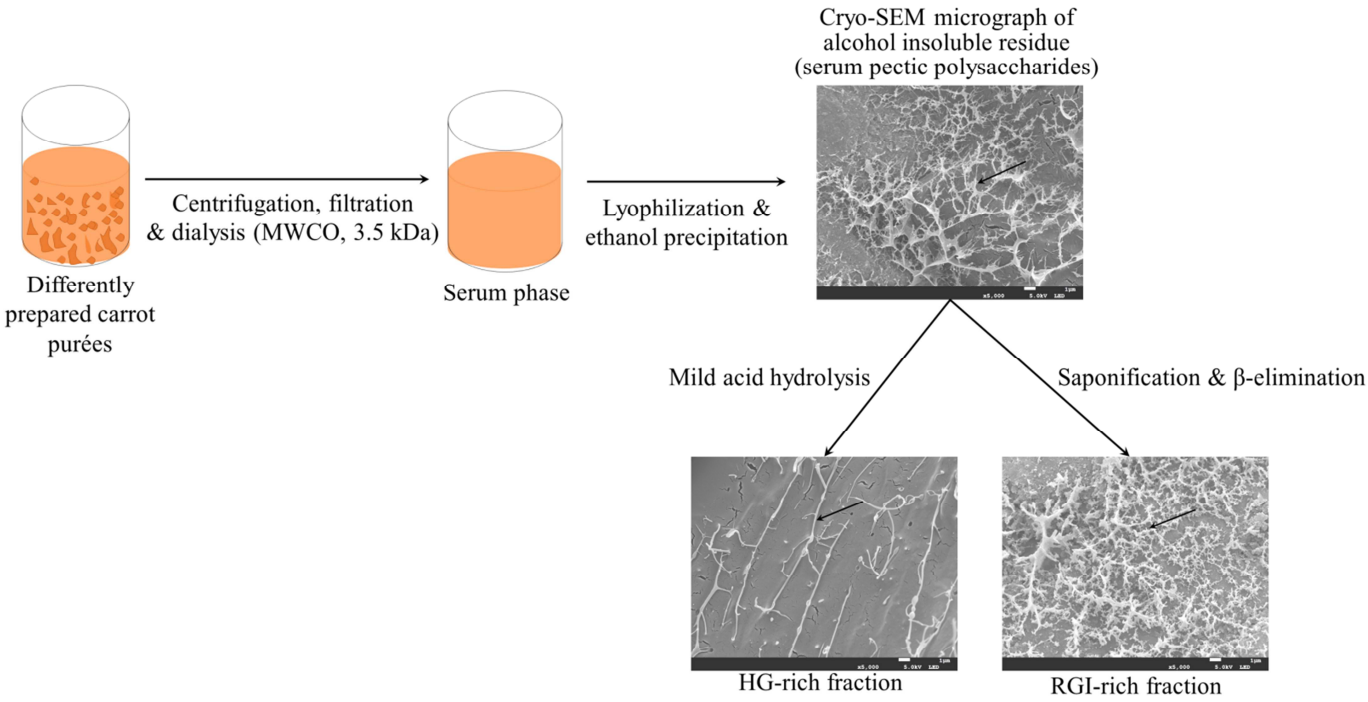

Highlights

- Serum pectin subdomains were isolated using hot acid and alkaline conditions.
- The AIR and derived RGI-rich fraction exhibited branch-like microstructures.
- Homogalacturonan-rich fractions displayed strand-like microstructures.

Unravelling the structure of serum pectin originating from thermally and mechanically processed carrot-based suspensions

Jihan Santanina J. Santiago[a], Clare Kyomugasho [a], Shashikant Maheshwari [a], Zahra Jamsazzadeh Kermani [a], Davy Van de Walle[b], Ann M. Van Loey [a], Koen Dewettinck[b] and Marc E. Hendrickx *[a]

[a]Laboratory of Food Technology, Leuven Food Science and Nutrition Research Centre (LFoRCe), Department of Microbial and Molecular Systems (M^2S), KU Leuven, Kasteelpark Arenberg 22, Box 2457, 3001 Leuven, Belgium

[b]Laboratory of Food Technology & Engineering, Faculty of Bioscience Engineering, Ghent University, Coupure Links 653, 9000 Gent, Belgium

*Corresponding author (telephone +32 16 321572; fax +32 16 321960; e-mail **marceg.hendrickx@kuleuven.be**).

Abstract

The molecular structure of pectin, a cell wall polysaccharide in fruits and vegetables, greatly determines its functionality. Owing to its solubility characteristics, pectin is naturally present in the particle and liquid (serum) phase of plant-based dispersions (e.g. purées) that can influence product functionality. The objective of the present study was to investigate the structure of serum pectin obtained from carrot purées, differently processed by a combination of mechanical tissue disintegration (blending and high pressure homogenization) and heat treatments (high and low temperature). Serum phases, isolated from the purées, were lyophilized and served as the starting material for isolation of the pectic polysaccharides as alcohol insoluble residues. Physico-chemical characterization revealed that different processing combinations of carrot purées can generate serum pectins with specific structural properties. Differences in the molecular weight of carrot serum pectic polysaccharides were observed depending on the sequence of heat and mechanical treatments. Subsequent partitioning of carrot serum pectic polysaccharides into rhamnogalacturonan I (RGI) and homogalacturonan (HG)-rich fractions using hot alkaline and mild acid conditions, respectively, revealed the composition and molecular characteristics of the serum pectin subdomains. The RGI-rich fractions were mainly characterized by high concentrations of neutral sugars (arabinose, galactose, and rhamnose) and exhibited branch-like structures in solution under cryo-SEM. HG-rich fractions, on the other hand, were characterized by highly linear galacturonic acid-rich pectin and exhibited strand-like structures under cryo-SEM. Knowledge of these structural changes can be useful in exploring the functionalities of carrot serum pectic polysaccharides.

Keywords

Carrot purée, serum pectin, homogalacturonan-rich fraction, rhamnogalacturonan I-rich fraction, microstructure

1. Introduction

The production of fruit and vegetable-based dispersions such as soups, smoothies, sauces and purées involves tissue disintegration and heat treatments, which alters the microstructure of the plant matrix resulting in a complex multi-scale food system structured by particles dispersed in a continuous (serum) phase (Moelants, et al., 2014). Pectin, due to its solubility characteristics, is present in both the particle and serum phase, and can exhibit different structural properties. Moreover, changes in the molecular structure of pectin in both phases can occur during processing and influence the functionality (e.g. flow behavior) of low-starch containing plant-based dispersions (Christiaens et al., 2012; Houben et al., 2014). Pectin solubilized in the serum phase, a water-soluble pectin termed as serum pectin, is suggested to be an important constituent of plant dispersions. Depending on its molecular characteristics, serum pectin is suggested to interact within the aqueous phase or with the particles and contribute to the overall structure organization of plant-based dispersions (Kyomugasho, Willemsen, Christiaens, Van Loey, & Hendrickx, 2015; Moelants et al., 2014; Moelants et al., 2012). However, in-depth knowledge and understanding of the specific molecular characteristics of serum pectin naturally present in plant-based food dispersions is still limited. An insight into the molecular properties of serum pectin and how these properties change under specific processing conditions might prompt the exploration of serum pectin's potential as a functional component.

To date, pectin is a well-recognized biopolymer comprising several polysaccharide domains with at least 17 different monosaccharides interconnected through more than 20 different linkages (Ridley, O'Neill, & Mohnen, 2001). Homogalacturonan (HG) and rhamnogalacturonans (mainly rhamnogalacturonans I and II) are the most abundant pectic polysaccharides. On the one hand, HG is a linear chain of 1,4 linked α-D-galacturonic acid (GalA) residues known as the "smooth" region. Its GalA residues can be methyl-esterified at

C-6 up to 70-80 % and O-acetylated at C-3 or C-2 depending on the plant source (Voragen, Coenen, Verhoef, & Schols, 2009). On the other hand, rhamnogalacturonan I (RGI) consists of a backbone of the repeating disaccharide [-α-D-GalA-1,2-α-L-Rha-1-4-]n and represents 20-35 % of pectin. RGI, the "hairy" region, is ramified with side chains of individual, linear or branched oligosaccharide residues attached at the C-4 of rhamnose residues (Voragen et al., 2009). Linear arabinan and (arabino)galactan are the predominant RGI side chains (Caffall & Mohnen, 2009). Recently, the galacturonic acid and rhamnose residues of the RGI subdomain of pectin extracted from okra pods were found to be O-acetylated (Alba, Laws, & Kontogiorgos, 2015; Sengkhamparn et al., 2009). The third substructure, rhamnogalacturonan II (RGII) accounts for about 10 % of total pectin and, is the most complex and conserved structure among the pectic polysaccharides. This substructure comprises of a backbone consisting of at least eight GalA residues with side branches of either structurally distinct disaccharides or oligosaccharides (Caffall et al., 2009; Mohnen, 2008).

The structure of individual pectin subdomains can be revealed by partitioning pectin chemically and/or enzymatically followed by a physico-chemical characterization. In this regard, Thibault, Renard, Axelos, Roger, & Crepeau (1993) isolated the homogalacturonan fraction of apple, beet and citrus pectins using mild acid hydrolysis at 80 °C for 72 h and its characterization revealed different sensitivities of the glycosidic linkages of these pectins to acid hydrolysis. Recently, mild acid hydrolysis at 80 °C for 24 h was shown to be sufficient in isolating the homogalacturonan fraction of different citrus pectins (Kaya, Sousa, Crepeau, Sorensen, & Ralet, 2014). Similarly, the homogalacturonan subdomain of tomato pectin from unripe pericarp was selectively isolated using mild acid hydrolysis at 80 °C for 24 h and then investigated using atomic force microscopy (Round, Rigby, MacDougall, & Morris, 2010). Moreover, to characterize the molecular properties of sugar beet pectin (SBP), Morris, Ralet, Bonnin, Thibault, & Harding (2010) selectively isolated the homogalacturonan and

rhamnogalacturonan I subdomains by different means. On the one hand, the homogalacturonan subdomain of SBP was isolated using mild acid hydrolysis at 80 °C for 72 h, while on the other hand, the rhamnogalacturonan subdomain was obtained by enzymatically degrading the homogalacturonan using fungal pectin methyl-esterase and different polygalacturonases (Morris et al., 2010). Given that mild acid hydrolysis for 72 h can degrade and influence the molecular weight of homogalacturonan, a combination of different enzymes including pectin methylesterase, rhamnogalacturonan hydrolase, galactanase and arabinanase were used to isolate the homogalacturonan of sugar beet, apple and lime pectins (Bonnin, Dolo, Le Goff, & Thibault, 2002). However, fragments of rhamnogalacturonan side chains were still present in the enzymatically isolated homogalacturonan fraction (Bonnin et al., 2002). Therefore, using either chemical or enzymatic means of partitioning the pectin subdomains might often be associated with residual amounts of one fraction in another.

As a first step in gaining insight into the molecular properties of serum (solubilized) pectin, the chemical means of partitioning the pectin subdomains was used in the present study. Serum pectin polysaccharides inherently present in thermally and mechanically processed fruits and vegetables (e.g. carrot purée) can be structurally more complex than commercially-prepared, purified or chemically extracted pectins. Different serum pectin molecular structures can be obtained, depending on the sequence of thermal and mechanical treatments or the action of endogenous pectin-related enzymes (e.g. pectin methylesterase) (Santiago, Christiaens, Van Loey, & Hendrickx, 2016; Santiago, Jamsazzadeh Kermani, Xu, Van Loey, & Hendrickx, 2017). Therefore, the present work aimed to gain an in-depth understanding of the molecular structure of serum pectin polysaccharides, isolated from differently processed carrot purées, by selectively partitioning the homogalacturonan and rhamnogalacturonan subdomains. These subdomains were subsequently characterized for

121 their degree of methyl-esterification, molecular weight and neutral sugar composition. On the
122 one hand, mild acid hydrolysis at 80 °C for 24 h was applied to obtain the homogalacturonan
123 (HG) subdomain while on the other hand, a hot alkaline condition (90 °C for 2 h) was
124 employed to isolate the rhamnogalacturonan I subdomain. To visualize the microstructure of
125 serum pectin polysaccharides (as alcohol insoluble residue) and the partitioned carrot serum
126 pectin subdomains in solution, cryo-scanning electron microscopy (cryo-SEM) was used.

127 **2. Materials and methods**

128 *2.1 Materials*

129 A batch of fresh carrots (*Daucus carota* cv. Nerac) from a local shop was washed,
130 peeled and cut into slices of approximately 0.5 cm thick. All chemical reagents used were of
131 analytical grade.

132 *2.2 Preparation of carrot purées and isolation of the serum phases*

133 A schematic overview of the purée preparation is provided in Figure 1. The
134 combinations of thermal and mechanical treatments, applied in producing three differently-
135 prepared purées, were aimed at creating distinct pectin molecular structures. High temperature
136 treatment (HT) at 95 °C for 30 min was applied to inactivate the enzymes and/or solubilize
137 pectin into the serum phase (Houben et al., 2014; Moelants et al., 2012), while low
138 temperature treatment (LT) at 60 °C for 40 min was aimed at stimulating the action of
139 endogenous pectin methyl-esterase (PME) to generate low methyl-esterified pectin
140 (Christiaens et al., 2012; Santiago et al., 2016). High pressure homogenization (HPH) at 100
141 MPa was applied to enhance pectin solubilization into the serum phase of the purées
142 (Moelants et al., 2012).

143 Briefly, carrot slices were vacuum-packed in polyethylene bags (DaklaPack®
144 Lamigrip Stand-up Pouch Transparent; 220 mm × 300 mm + 65 mm bottom fold) and then
145 either heat treated at 95 °C for 30 min or left untreated (raw). De-mineralized water in a 1:1

(*w/w*) ratio was then added to the raw or heat treated carrot slices followed by mechanical disruption for 20 s at low speed then 40 s at high speed using a kitchen blender (Waring Commercial, Torrington, Connecticut, USA). Afterwards, a high pressure homogenizer (Panda 2 K, Gea Niro, Parma, Italy) was used at 100 MPa (single pass) to intensively disrupt the tissues. The purée obtained from the raw carrot slices was immediately vacuum-packed in polyethylene bags and either immediately subjected to HT at 95 °C for 30 min to inactivate pectin-modifying enzymes or first subjected to LT at 60 °C for 40 min to activate PME prior to an inactivation step (HT) as shown in Figure 1. After HT, samples were cooled to ambient temperature in an ice-water bath. In order to obtain and isolate the serum phase from the particles, the purées were centrifuged at 12,400 x g for 30 min at 20 °C (J2-HS centrifuge, Beckman, CA, USA). The serum phase, the supernatant, was vacuum-filtered, extensively dialyzed (3.5 kDa, MWCO) against de-mineralized water, lyophilized using Christ alpha 2-4 freeze dryer (Osterode, Germany) and then stored in a desiccator over P_2O_5 until further use. Hereto, the dry material obtained after freeze-drying the serum is referred as the lyophilized serum and served as the starting material for isolation of the carrot serum pectic polysaccharides, as alcohol insoluble residue.

2.3 Isolation of carrot serum pectic polysaccharides as alcohol insoluble residue (AIR)

Approximately 1.2 g of lyophilized serum, from each of the differently-prepared carrot purées, was suspended in 600 mL of 95 % (*v/v*) ethanol and mixed for 30 min at 4 °C. The resulting suspension was vacuum-filtered (Machery-Nagel MN 615, Ø 90 mm) and re-suspended in 300 mL of 95 % (*v/v*) ethanol. After a second vacuum filtration step, the alcohol insoluble residue (AIR) was suspended and stirred in acetone. A final vacuum filtration generated the AIR which was dried overnight at 40 °C, thoroughly mixed and stored in a desiccator over P_2O_5 until further analysis.

2.3.1 Isolation of the rhamnogalacturonan I (RGI)-rich fraction from AIR using hot alkaline conditions

AIRs of lyophilized sera, from differently-prepared carrot purées, were subjected to alkaline pH and high temperature conditions. Approximately 60 mg AIR was suspended in 12 mL de-mineralized water and stirred at 4 °C for 16 h. Subsequently, the samples were heated at 90 °C for 30 min and hot sodium hydroxide (1 M) was gradually added until pH 12 (pH meter Lab 860, Schott Instruments Analytics GmbH, Germany). The samples were kept at 90 °C for 2 h with mild stirring and afterwards cooled to ambient temperature. Subsequently, ethanol was added until a final concentration of 80 % (*v/v*) and the suspension was vacuum-filtered using 0.1 μm (Durapore® membrane filters, Merck Millipore ltd. Ireland) glass unit filter. The residue/precipitate was dissolved in 10 mL de-mineralized water, neutralized to pH 6 using 0.1 M hydrochloric acid and consequently dialyzed (MWCO, 3.5 kDa) against de-mineralized water for 48 h. Finally, the suspensions/RGI-rich fractions were lyophilized and then stored in a desiccator over P_2O_5 until further analysis.

2.3.2 Isolation of the homogalacturonan (HG)-rich fraction from de-esterified AIR using mild acid hydrolysis

AIRs were first subjected to chemical de-esterification and then acid hydrolysis based on the work of Morris et al. (2010) and Thibault et al. (1993) with minor modifications. De-esterification/saponification of serum pectic polysaccharides was aimed at increasing the resistance of the linkages of galacturonic acid residues to hydrolysis under the high temperature and acid conditions (Thibault et al., 1993). To this extent, approximately 60 mg AIR was suspended in 12 mL de-mineralized water and stirred at 4 °C for 16 h. Cold sodium hydroxide (1 M) was slowly added to the mixture until a pH of 12 was obtained and then maintained for 6 h at 4 °C. After chemical de-esterification, the pH was adjusted to 1.0 using hydrochloric acid (1 M) and the samples were subsequently heated in a temperature-

controlled oil bath at 80 °C for 24 h. After cooling the samples to ambient temperature, ethanol was added until a final concentration of 80 % (*v/v*). The suspension was subsequently vacuum-filtered using a 0.1 μm (Durapore® membrane filters, Merck Millipore ltd. Ireland) glass unit filter. About 3 mL of 0.1 M HCl was gradually added to the residues obtained followed by 10 mL de-mineralized water. Finally, the samples/HG-rich fractions were neutralized to pH 6 using 0.5 M lithium hydroxide, extensively dialyzed (MWCO, 3.5 kDa) against de-mineralized water and lyophilized prior to being stored in a desiccator over P_2O_5 until further.

2.4 Analysis of the physico-chemical characteristics of carrot serum pectic polysaccharides and partitioned serum pectin subdomains

2.4.1 Monosaccharide composition

Monosaccharides including neutral sugars, galacturonic and glucuronic acids were determined as described by De Ruiter, Schols, Voragen & Rombouts (1992) and Nagel, Sirisakulwat, Carle, & Neidhart (2014) with minor modifications. Methanolysis followed by acid hydrolysis of each sample was carried out to obtain and analyze the constituting monosaccharides. The resulting monosaccharides were identified and quantified using high performance anion exchange chromatography (HPAEC) combined with pulsed amperometric detector (PAD). Briefly, 1 mg sample was dissolved in 1 mL de-mineralized water and an aliquot of 20 μL was dried in a screw cap test-tube under a N_2 evaporator at 45 °C. After adding 0.5 mL anhydrous 2 M methanolic HCl, methanolysis was carried out at 80 °C for 16 h in an oil bath. The samples were then cooled to ambient temperature and dried under N_2 at 30 °C. Subsequently, acid hydrolysis using 0.5 mL of 2 M trifluoroacetic acid (TFA) was performed for 1 h at 121 °C. The acid hydrolyzed samples were cooled to ambient temperature, dried under N_2 evaporator at 45 °C to remove the TFA and then dissolved in ultrapure water (organic free, 18 MΩ cm resistance) to a final concentration of 0.002 % (*w/v*).

To correct the possible degradation of monosaccharides, 100 µL aliquots of a mixture of sugar standards (L-fucose, L rhamnose, L-arabinose, D-galactose, D-glucose, D-mannose, D-xylose, galacturonic acid and glucuronic acid) with known concentrations were subjected to methanolysis and TFA hydrolysis. All the samples were filtered through 0.45 µm (Chromafil A-45/25, 0.45 µm, Macherey-Nagel Gmbh, Duren, Germany) prior to injection onto HPAEC. A Dionex HPLC system (DX600), equipped with a GS50 gradient pump, a CarboPac™ PA20 column (150 x 3 mm, pH range = 0-14), a CarboPac™ PA20 guard column (30 x 3 mm), and an ED50 electrochemical detector (Dionex, Sunnyvale, USA) was used. The detector was equipped with a reference pH electrode (Ag/AgCl) and a gold electrode that was used in the PAD mode, performing a quadruple potential waveform. The elution gradients were adapted from the method described by (Arnous & Meyer, 2008). After equilibration (-10 → -5 min: 100 mM NaOH, -5 → 0 min: elution gradient), 10 µL hydrolysate was injected and eluted at 30 °C with a flow rate of 0.5 mL/min. From 0 to 20 min, elution gradients of 0.5 mM NaOH to obtain better peak resolution of xylose and mannose or 15 mM NaOH to separate the peaks of rhamnose and arabinose were applied (Jamsazzadeh Kermani et al., 2014). The column was regenerated by using 500 mM NaOH (20 → 30 min). To quantify the monosaccharides, mixtures of un-hydrolyzed sugar standards were used at varying concentrations (*i.e.* 5-25 ppm galacturonic acid and 1-10 ppm for neutral sugars and glucuronic acid). Peak areas of un-hydrolyzed and hydrolyzed sugar standards were compared and the recovery values were taken into account in quantifying the monosaccharides. All hydrolysis and chromatographic measurements were carried out in duplicate.

2.4.2 Degree of methyl-esterification

The degree of methyl-esterification (DM) was analyzed based on the method of Kyomugasho, Christiaens, Shpigelman, Van Loey, & Hendrickx (2015) using Fourier

transform infra-red (FT-IR) spectroscopy (ATR-FTIR, Shimadzu FTIR-8400S, Japan). The transmittance of the samples was recorded at wavenumbers from 4000 cm^{-1} to 400 cm^{-1} at resolution 4 cm^{-1}, peak intensities at 1600-1630 cm^{-1} due to carboxylate group (COO^-) and at 1740 cm^{-1} due to methyl-ester carbonyl group (C=O) stretching being of interest. The ratio (*R*) between the peak intensity at 1740 cm^{-1} and the sum of the peak intensities at 1740 cm^{-1} and 1600-1630 cm^{-1} was used to predict the DM of the samples based on the calibration line: DM (%) = 136.86 x *R* + 3.987 (Kyomugasho, Christiaens, et al., 2015). The calibration line was constructed using citrus pectin with different DMs (0-94 %) obtained enzymatically/chemically as well as another set of DMs (0-94 %) generated by mixing polygalacturonic acid and high DM citrus pectin in different ratios (Kyomugasho, Christiaens, et al., 2015).

2.4.3 Protein content

The total nitrogen content of the samples was measured using an EA 1110 CHNS-O elemental analyzer (CE-Instruments/Thermo Fisher Scientific). About 1 mg of the sample was placed in a crimped tin capsules (8 mm × 5 mm) prior to combustion in the elemental analyzer. A conversion factor of 6.25 was used to calculate the amount of proteins in the sample (Immerzeel, Eppink, de Vries, Schols, & Voragen, 2006).

2.4.4 Molecular weight distribution and intrinsic viscosity

The molecular weight distribution and intrinsic viscosity of the samples were analyzed based on the work of Shpigelman, Kyomugasho, Christiaens, Van Loey, & Hendrickx (2014). A high performance size exclusion chromatography (HPSEC) integrated to 4 detectors, namely: PN3621 multi-angle laser light scattering (MALLS) from Postnova analytics, Germany; Shodex RI refractive index (RI) from Showa Denko K.K., Kawazaki, Japan; a PN 3310 viscometer from Postnova analytics, Germany and a G1316A diode array detector (DAD) from Agilent technologies, Diegem, Belgium that qualitatively detects the presence of

UV absorbing molecules, was used. Prior to HPSEC analysis, the samples were dissolved and prepared differently as they showed different filterability and recovery after filtration. However, all the samples were eluted using the same buffer and analytical conditions. The AIRs and RGI-rich fractions (0.2 % *w/v*) were stirred overnight in a pH 4.4 buffer (0.1 M acetic acid and $NaNO_3$) followed by filtration through a 0.45 μm syringe filter (Miller-HV). For the de-esterified AIRs and HG-rich fractions, 0.2 % (*w/v*) sample was first dissolved in ultrapure (organic free, 18 MΩ cm resistance) water overnight followed by dialysis (MWCO, 3.5 kDa) against 0.05 M $NaNO_3$ solution for 48 h. To facilitate the filterability, these samples, were heated at 50 °C for 10 min prior to filtration (Thibault et al., 1993). Exactly 100 μL of filtered sample was then injected using an auto-sampler onto a series of three Waters column (Waters, Milford, MA), namely, Ultrahydrogel 250, 1000 and 2000 with exclusion limits of 8×10^4, 4×10^6, and 1×10^7 g/mol, respectively. A constant flow rate of 0.5 mL/min of the elution buffer (0.1 M acetic acid and $NaNO_3$ buffer at pH 4.4) was applied and the columns were kept at 35 °C. A dn/dc value of 0.146 mL/g was used to calculate the concentration. The molecular weight was calculated using the Debye fitting method (up to 2^{nd} order) by the software provided by the manufacturer of MALLS detector (NovaMals, version 1.2.0.0, Postnova analytics, Germany). The intrinsic viscosity was obtained from the viscometer detector signals and the calculated concentration of the samples. All the samples were analyzed in duplicate.

2.5 Visualization of the microstructure of carrot serum pectin polysaccharides (AIRs) and derived pectin subdomains

Cryo-scanning electron microscopy (cryo-SEM) was used to visualize the microstructure of carrot serum pectic polysaccharides in solution. Approximately 1 mg of lyophilized sample was dissolved overnight in 1 mL ultrapure water (organic free, 18 MΩ cm resistance). A few drops of the sample was placed onto a slot on a stub with rivets, vitrified

and transferred into the cryo-stage at -140 °C in the cryo-preparation chamber (PP3010T cryo-SEM preparation system, Quorom Technologies, UK). The sample was freeze-fractured, sublimated at -90 °C for 25-30 min under controlled vacuum conditions and then sputter coated with platinum using argon gas to prevent charging during electron beam targeting (Kyomugasho et al., 2016). Finally, the sample was transferred onto the SEM stage and examined using a JEOL JSM 7100F SEM (JEOL Ltd, Tokyo, Japan) for their microstructure in solution.

2.6 Data analysis

To determine the statistical significance, duplicate means were analyzed by one-way analysis of variance using JMP statistical software (JMP Pro 13.0.0, SAS Institute Inc.). A student's t-test was used to compare significantly different (p-value <0.05) mean values of only two groups (i.e. between starting material and derived fraction), while a post-hoc test using Tukey's honest significant difference (HSD) was employed for mean values of more than two groups (i.e. among starting materials or derived fractions).

3. Results and discussion

3.1 Molecular properties of RG I-rich fractions and their respective carrot serum pectic polysaccharides (AIRs)

3.1.1 Monosaccharide composition

First, it can be seen that the AIR of HT+HPH contained a higher amount of total sugars and pectin-associated sugars compared to the AIRs of HPH+HT and HPH+LT+HT (Table 1). This suggests solubilization of distinct pectic polysaccharides into the serum phase depending on the combinations of thermal (*i.e.* high and low) and mechanical treatments applied in preparing the purées (Santiago et al., 2016). High concentrations of galacturonic acid (GalA) as well as considerable amounts of rhamnose (Rha), arabinose (Ara), galactose (Gal) and glucose (Glu) were detected in the alcohol insoluble residues (AIRs), while trace amounts of fucose (Fuc), xylose (Xyl), mannose (Man) and glucuronic acid (GlucA) were

found. Among the monosaccharides, Glu and Man have been identified as non-pectin associated sugars which possibly originate from residual starch, glucomannan and non-crystalline cellulose (Houben, Jolie, Fraeye, Van Loey, & Hendrickx, 2011; Massiot, Rouau, & Thibault, 1988). The presence of these non-pectic sugars in carrot serum was also reported by Kyomugasho, Willemsen, et al. (2015).

Looking at the RGI fractions, based on the weight of the recovered residues over the amount of the starting materials, the percentage isolation yield of the RGI-rich fractions was about 33.1 % for HT+HPH, 27.5 % for HPH+HT and 36.6 % for HPH+LT+HT. It was observed that significantly (p-value <0.05) lower concentrations of Glu and Man were exhibited by all the RGI-rich fractions compared to their corresponding initial materials (AIRs), as presented in Table 1. This suggests the degradation and solubilization of Glu and Man containing non-pectic polysaccharides. Besides the decrease in Glu content, remarkably lower concentrations of GalA were observed in all the RGI-rich fractions. The concentration of GalA that remained in the RGI-rich fractions was approximately 16-18 % (*w/w*) of the amount of GalA in the initial samples implying that about 82-84 % (*w/w*) of GalA present in the initial material was degraded and solubilized. β-elimination reaction of methyl-esterified GalA residues of the homogalacturonan subdomain has been reported as the main mechanism of pectin degradation at alkaline pH and high temperature conditions (Sila et al., 2009).

Furthermore, the extent of GalA content reduction among the RGI-rich fractions relative their respective AIRs was comparable suggesting a relatively similar susceptibility of their homogalacturonan to degradation under the given conditions. Given that the mole ratio of the remaining GalA to Rha was too high to represent only RGI, a repeating disaccharide of [→4)-α-D-GalA-(1→2)-α-L-Rha-(1→] (O'Neill, et al., 1996), the remaining GalA could probably also originated from RGII as its backbone is made up of GalA as well as residual HG. In the current work, 59-64 % (*w/w*) of the initial Rha concentration was retained while

346 63-69 % (*w/w*) Ara and 68-75 % (*w/w*) Gal were also found in the RGI-rich fractions.
347 Nevertheless, the considerable amounts of Rha, Ara and Gal compared to other sugars,
348 particularly GalA, indicates the presence of rhamnogalacturonan-rich serum pectin,
349 irrespective of the serum type obtained from different carrot purée preparations. Arabinose-
350 and galactose-containing polysaccharides covalently attached as side chains to rhamnose are
351 recognized structural components of RGI pectic subdomain (Voragen, Beldman & Schols,
352 2001; Endress, Mattes & Norz, 2006).

353 *3.1.2. Sugar ratios: extent of branching of AIRs and their derived RGI fractions*

354 To obtain information on a molecular level, the monosaccharide composition data was
355 used in calculating the molar ratios between pectin-related sugars (Houben et al., 2011). An
356 insight into the structural variations of the RGI-rich fractions compared to their AIRs is
357 presented in Table 2a. The molar ratio of GalA to the sum of Fuc, Rha, Ara, Gal and Xyl
358 describes the linearity of serum pectin, with a high value suggesting the presence of more
359 linear pectin/HG-rich pectin; while the molar ratio of the sum of Ara and Gal to Rha provides
360 a global view of the extent of branching of RGI in which a high value suggests that the
361 branching point (Rha) largely contains sugar side chains rich in Ara and Gal. To determine
362 the contribution of RG to the pectin population, the molar ratio between Rha and GalA was
363 also determined (Houben et al., 2011; Kaya et al., 2014). In this context, it can be observed
364 that AIRs of HT+HPH and HPH+HT samples contained more linear and less branched pectin
365 compared to the AIR from the HPH+LT+HT sample which exhibited a higher degree of RGI
366 branching. This suggests structural variations among the initial serum pectic polysaccharides
367 due to different processing combinations used in preparing the carrot purées which is
368 consistent with our previous work (Santiago, et al., 2016). Moreover, comparing the AIRs
369 with their derived RGI-rich fractions, a large difference in the linearity of pectin is noticeable
370 due to the previously observed degradation of homogalacturonan chains and consequent loss
371 of GalA. By contrast, the extent of branching of RGI remained comparable in both RGI-rich

fractions and initial materials. This observation is supported by the higher proportion of Rha to GalA in the RGI-rich fractions indicating a large contribution of RGI polysaccharides (Table 2a). Regardless of the process combinations used to generate the starting serum pectic polysaccharides, it can be deduced that the RGI-rich fractions isolated had very low amounts of GalA-rich chains, while maintaining the branched RGI subdomain. This clearly suggests that linkages between neutral sugars (both in the backbone and side chains) were less prone to degradation under hot alkaline condition.

3.1.3 Degree of methyl-esterification

The degree of methyl-esterification (DM) of pectin, defined as the number of moles of methyl esters per 100 moles of galacturonic acid residues, is an important characteristic attributed to the linear homogalacturonan subdomain (Voragen et al., 2001). The serum pectic polysaccharides from different processes (AIRs) contained high methyl-esterified GalA residues ranging from 52 % to 65 %, as shown in Table 2a. The AIR of the HPH+LT+HT sample had a significantly (p <0.05) lower DM (~52 %) due to the action of endogenous pectin methyl-esterase (Santiago et al., 2016), that was deliberately stimulated during the carrot purée preparation (Figure 1). On the other hand, RGI-rich fractions derived from these AIRs exhibited comparable very low DMs of 4.4 % to 5.6 %. These values are in close agreement with the low DM (6 %) of rhamnogalacturonan-rich pectin isolated from carrot tissues through an enzymic liquefaction process (Schols & Voragen, 1994). In the current work, the observed low DM (due to residual methyl esters) in the RGI-rich fractions is mainly attributed to the loss of methyl-esterified GalA units owing to the base-catalyzed splitting of the homogalacturonan chains via a β-elimination reaction (Sila et al., 2009). The residual methyl esters may be attributed to other substructures, since the GalA residues of the RGI backbone are presumably not methyl-esterified (Kravtchenko, Arnould, Voragen, & Pilnik, 1992). Given that complete isolation of the HG was not achieved (as the rate of β-elimination is retarded, as the reaction proceeds due to decreased DM), the RGI-rich fractions were

probably associated with residual HG and/or RGII subdomains. The methyl groups can therefore be attributed to RGII which can be methyl-esterified at the C-6 position (Ishii et al., 1999) or presence of residual homogalacturonan chains with methyl-esterified GalA units.

3.1.4 Molecular weight distribution and intrinsic viscosity

The size exclusion elution profiles showing the RI, LS 92° and UV 280 nm signals of the RGI-rich fractions and their corresponding initial material (AIRs) are presented in Figure 2. From the concentration profiles, it can be observed that all the pectic polymers of the initial samples (AIRs) were eluted earlier, starting at ~38 min while polymers of RGI-rich fractions eluted later, starting at ~44 min (Figure 2A). This elution time difference suggests a change in the hydrodynamic volume of the polymers after subjecting the serum pectic polysaccharides (AIRs) to hot alkaline conditions, due to degradation of the HG subdomains. The polymers of RGI-rich fractions presented smaller hydrodynamic volumes than their respective AIRs. Furthermore, the AIR of the HT+HPH sample showed a significantly (p <0.05) higher M_w compared to AIRs of HPH+HT and HPH+LT+HT samples, indicating the solubilization of different pectic populations into the serum phase during the purée preparation. By contrast, the concentration peak profiles of the RGI-rich fractions appeared identical and their M_w were also relatively comparable (Table 2b). The M_w of RGI-rich fractions were significantly (p <0.05) lower than their respective initial materials (AIRs) for both the high and low molecular weight polymer populations. The polydispersity indices of the different AIRs ranged from 1.21 to 1.90, while slightly lower polydispersity indices (1.18-1.36) were observed in the RG-rich fractions. As previously discussed that carrot serum pectin had high degree of branching, a comparison of its M_w to a commercial pectin reported to be highly branched (sugar beet pectin) is made in this section. The average M_w (108 ± 11 kDa) of the RGI-rich fractions of carrot serum pectic polysaccharides was lower compared to the M_w (188 kDa) of sugar beet pectin RGI fraction (Morris et al., 2010). Besides the difference due to botanical source,

423 isolation procedures used in obtaining the RGI fractions can be attributed to these M_w
424 differences. In the aforementioned study, the homogalacturonan region of sugar beet pectin
425 was enzymatically hydrolyzed to obtain the RGI fraction in contrast to the use of chemical
426 means employed in the present study.

427 In terms of intrinsic viscosity, as AIR of HT+HPH sample had very high M_w polymers
428 (in high concentration), a high intrinsic viscosity was observed. However, the AIR of
429 HPH+HT sample that had significantly lower M_w polymers than AIR of the HT+HPH sample
430 showed comparable intrinsic viscosity that can be due to their relatively comparable
431 molecular structures (*cf.* Table 2a, 2b). The alcohol insoluble residue with the lowest M_w and
432 being rich in neutral sugar side chains (HPH+LT+HT) showed the lowest intrinsic viscosity
433 (Table 2). Neutral sugar-rich pectins was found to have lower intrinsic viscosity which can be
434 due to the presence of highly dense and spherical polymers that might either be branched
435 pectin molecules or relatively stable aggregates (Kravtchenko, Voragen & Pilnik, 1992).
436 Moreover, from the UV 280 nm profile, a peak from ~58 min elution time is noticeable and
437 could be due to UV absorbing compounds such as proteins and polyphenols (Figure 2B). In
438 fact, according to Christiaens et al. (2015), the absorbance at 280 nm was attributed to
439 proteins, which were presumed to be attached to the high M_w polymers of water-soluble pectin
440 of carrot-derived waste streams. To confirm the presence (absence) of proteins, in the current
441 study, the protein content was determined based on the total nitrogen content of the samples
442 and ranged from 7.2 % to 13.4 % for the AIRs and, 1.2 % to 3.2 % for the RGI-rich fractions
443 (Table 2a). This possibly indicates that proteins could be associated with the neutral sugar
444 side chains of carrot pectin (Immerzeel et al., 2006), but not all detected proteins could be
445 attached to pectin especially in the AIRs. Proteins detected in commercial pectins such as
446 apple and lemon pectins were found to be mainly present in the neutral sugar side chains
447 (Kravtchenko, Penci, Voragen & Pilnik,1993).

448 *3.2 Molecular properties of HG-rich fractions and their respective de-esterified AIR*

449 *3.2.1 Monosaccharide composition*

450 Based on the weight of the material recovered from the starting AIRs, the isolation
451 yields of the HG-rich fractions were about 43.4 %, 42 % and 44.9 % (*w/w*) for HT+HPH,
452 HPH+HT and HPH+LT+HT serum samples, respectively. The monosaccharide composition
453 of the HG-rich fractions differed from their respective de-esterified AIRs (Table 3). Low to
454 trace amounts of Rha, Ara and Gal were detected in the HG-rich fractions. In comparison to
455 the respective initial sugar content of the de-esterified AIR, the HG-rich fractions retained
456 Rha ranging from 26-30 % (*w/w*), Ara from 0-2 % (*w/w*) and Gal from 11-16 % (*w/w*). This
457 suggests the degradation of the linkages of neutral sugar side chains as well as most of the
458 rhamnogalacturonan I backbone of the carrot serum pectic polysaccharides. This also shows
459 that Ara-containing side chains of carrot serum pectic polysaccharides were the most labile to
460 acid followed by Gal, which is in agreement with the results on the mild acid hydrolysis of
461 commercial pectins from apple, sugar beet, citrus (Kaya et al., 2014; Morris et al., 2010;
462 Thibault et al., 1993; De Vries et al., 1983) and pectin from the pericarp of unripe tomato
463 (Round et al., 2010). Moreover, an average of 87 % (*w/w*) of the initial GalA concentration
464 was recovered in the HG-rich fractions, which evidenced the isolation of the
465 homogalacturonan-rich carrot serum pectin. The HG-rich fractions obtained had about 89.4 to
466 92.0 mol % of GalA (Table 3), indicating a higher concentration of GalA to the total pectin-
467 related sugars compared to the de-esterified AIR (57.8-67.1 mol % of GalA). This shows that
468 GalA linkages of carrot serum pectic polysaccharides were less susceptible to degradation
469 under mild acid condition compared to the RGI subdomain, which is in agreement with the
470 previous findings of several researchers (Kaya et al., 2014; Morris et al., 2010; Round et al.,
471 2010; Thibault et al., 1993).

3.2.2. Degree of methyl-esterification and sugar ratios of de-esterified AIRs and HG-rich fractions

The de-esterified AIRs and HG-rich fractions exhibited comparable low DM values ranging from 5.7 to 8.6 % (Table 4a), indicating that the mild acid conditions used to generate the HG-rich fractions did not induce further chemical de-methoxylation. These DM values are in close agreement with the DM of de-esterified and acid hydrolyzed sugar beet (5 %), apple (3 %) and citrus pectin (3 %) (Thibault et al.,1993).

To assess the linearity and the contribution of RG to pectin population as well as the extent of RGI branching, the molar ratios of pectin-related sugars were evaluated as discussed previously (*cf.* section 3.1.2). First, it must be noted that AIR and de-esterified AIR showed similar sugar ratio trends for all the serum types, which suggests that subjecting the AIR to alkaline conditions for 6 h at 4 °C did not alter other structural properties of serum pectic polysaccharides, except the DM (*cf.* Table 2a and Table 4a). Hence, the de-esterified AIRs which served as starting material for isolation of HG-rich fractions were comparable to the starting material (AIR) for isolation of RGI-rich fractions.

Comparing the de-esterified AIRs and HG-rich fractions, the former presented less linear and more branched serum pectic polysaccharides (Table 4a). By contrast, HG-rich fractions exhibited a lower concentration of the major pectin-related neutral sugars (Rha, Ara and Gal) that consequently resulted in a reduction of their degree of RGI branching. Moreover, the HG-rich fractions were highly linear as represented by high values of the sugar ratios representing the linearity of pectin. This evidenced the degradation of neutral sugar side chains as well as the RGI backbone of de-esterified AIRs. The results indicated the substantial loss of the RGI subdomain of carrot serum pectic polysaccharides under the given acid condition, however, a fragment of the RGI backbone was possibly still present in the GalA-rich fraction. Specifically, the HG-rich fraction of the HPH+LT+HT sample (initially having

the highest degree of RGI branching) showed a considerable molar ratio of Ara and Gal to Rha compared to the other HG-rich fractions (Table 4a). This could possibly be due to the observed higher initial degree of RGI branching of this specific sample (HPH+LT+HT) which probably required longer hydrolysis time (Thibault et al., 1993).

3.2.3 Molecular weight distribution and intrinsic viscosity

Differences in the molecular weight and intrinsic viscosity of the HG-rich fractions and their respective de-esterified AIRs were observed. Comparing all the different initial materials (de-esterified AIRs), different peak profiles and molecular weights were detected (Figure 3). These varying peak profiles can be related to the previously observed different structural properties (e.g. linearity and degree of RGI branching) and possible differences on the conformation of serum pectic polysaccharides in solution. Comparing the de-esterified AIRs with their respective HG-rich fractions, differences in the peak maximum of their concentration curves can be distinguished (Figure 3A). The peak maxima of the concentration curves of HG-rich fractions were situated at around ~55 min, while the peak maxima of de-esterified AIRs were observed between ~50 to 52 min. This indicates that a high population of polymers in the HG-rich fractions had smaller hydrodynamic volume compared to the polymers of de-esterified AIRs. Moreover, the HG-rich fractions were generally characterized by lower M_w pectic polymers (compared to AIRs) with two polymer populations, one eluting at approximately 42-48 min (population I) and the other at 48-62 min (population II). For population I, the very high M_w values obtained can be possibly due to aggregated polymers. These high apparent M_w polymers comprised less than 10 % of the injected total mass fraction which can be due to the aggregation of some pectic polymers, given the high linearity of pectin (Table 4b), very low DM, hence high sensitivity to divalent ions (Shpigelman et al., 2014). For polymer population II, low M_w pectic polymers comprising more than 50 % of the total mass fraction (Table 4b). Given its high concentration, this population of low M_w pectic

polymers can be considered as the representative M_w values of the HG-rich fractions, which is in close agreement with the values of 17 kDa- 37 kDa for the homogalacturonan fraction of citrus pectins (Kaya et al., 2014; Yapo et al., 2007) and 17 kDa- 22 kDa for sugar beet pectins (Morris et al., 2010; Thibault et al., 1993) obtained by mild acid hydrolysis. In the present study, the polydispersity indices of the isolated HG-rich fractions, being 1.03 to 1.14 for polymer population II (the most abundant population), suggested a relatively more homogenous M_w distribution of polymers compared to the de-esterified AIR with polydispersity indices of 1.28-1.98.

Furthermore, although the de-esterified AIRs exhibited higher M_w, they presented relatively lower intrinsic viscosities particularly for the high M_w polymer population compared to the HG-rich fractions. Specifically, the intrinsic viscosities of HG-rich fractions of HT+HPH and HPH+HT samples eluted at 44 to 48 min were 1.39 dL/g and 1.79 dL/g, respectively, which are higher than the intrinsic viscosities of their corresponding de-esterified AIRs, being 0.84 dL/g and 0.94 dL/g. This can probably be explained by their different hydrodynamic volumes and structural properties, in which the de-esterified AIRs were characterized by more branched pectic polymers and probably suggesting higher flexibility in solution leading to low intrinsic viscosity. Polymer population II of the HG-rich fractions, predominantly containing high concentration of low M_w polymers, had an intrinsic viscosity of 0.34-0.46 dL/g, which are relatively lower than the intrinsic viscosity of 0.70-1.16 dL/g for acid hydrolyzed citrus and sugar beet pectins (Kaya et al., 2014; Morris et al., 2010; Yapo, Lerouge, Thibault, & Ralet, 2007; Thibault et al., 1993). The lower intrinsic viscosity of the homogalacturonan-rich fractions observed in the current work can probably be attributed to the presence of RGI fragments. Polymer flexibility, which is reported to influence the intrinsic viscosity (Kravtchenko et al., 1992), increases with HG-rich fractions containing fragments of RGI than HG fractions that are almost entirely free from branched

rhamnogalacturonan I. Aggregation and high polydispersity of pectic polymers can also influence the M_w and intrinsic viscosity values (Endress, Matess & Norz 2006). Moreover, the UV 280 nm profiles generally showed a peak from ~58 min which can be due to proteins and other UV-absorbing molecules such as polyphenols (Figure 3B). In fact, the de-esterified AIRs had a protein content ranging from 4.9-8.2 %, while the HG-rich fractions had 1.5-3.3 % protein (Table 4a). The protein detected in HG-rich fractions was probably associated with the residual RGI subdomain after acid hydrolysis and dialysis.

3.3 Microstructure of carrot serum AIRs and the partitioned subdomains

AIRs of the lyophilized serum obtained from differently-prepared carrot purées, and their partitioned subdomains were viewed under a cryo-SEM to further investigate their microstructure in solution. Figure 4 shows representative cryo-SEM micrographs of 0.1 % solutions of alcohol insoluble residues (AIRs), RGI- and HG-rich fractions. In the micrographs, white branch-like and/or strand-like structures can be observed and are mostly composed of pectic polymers together with a little vitreous ice. Specifically, the different AIRs are composed of branch-like structures. Although the AIRs of the HT+HPH and HPH+LT+HT samples were previously shown to compose of serum pectic polysaccharides with different M_w, degree of RGI branching and DM, there was no clear/distinguishable differences in their microstructures under cryo-SEM. The RGI-rich fraction of HT+HPH sample exhibited a dense population of short branch-like structures compared to its AIR as well as to the RGI-rich fraction of HPH+LT+HT (Figure 4). In terms of the HG-rich fractions, the HT+HPH sample showed more visible long strand-like features with limited branch-like structures (if any). Furthermore, comparing the different AIRs with their respective RGI and HG-rich fractions, more distinguishable structural features can be identified. The microstructures of the AIRs are comparable to their respective RGI-rich fractions owing to the branch-like features. By contrast, the HG-rich fractions exhibit strand-like structures with no

branch-like features. These cryo-SEM micrographs show that AIRs and RGI-rich fractions of can exhibit comparable microstructures in solutions, which are different from microstructures exhibited by HG-rich fractions, an observation that can be greatly attributed to their overall structure differences. Carrot serum pectic polysaccharides is composed of highly branched pectic populations; which is in agreement with our physico-chemical characterization results as well as the findings of Houben et al. (2011).

Conclusion

Different processing combinations, applied in preparing the carrot purées, can be used to create distinct molecular structures of serum (solubilized) pectic polysaccharides. High temperature treatment of carrot pieces followed by blending and high pressure homogenization resulted in high concentration of serum pectin with high M_w, DM and linearity. Furthermore, the structure of serum pectic polysaccharides, isolated from the serum phase of differently-processed carrot purées, was successfully partitioned into its constituting rhamnogalacturonan I and homogalacturonan subdomains through selective chemical hydrolysis. On the one hand, a rhamnogalacturonan I-rich fraction, mainly characterized by a high concentration of rhamnose, arabinose and galactose, was obtained by subjecting the serum pectic polysaccharides to hot alkaline conditions to selectively degrade the homogalacturonan subdomain. On the other hand, a homogalacturonan-rich fraction of, highly linear galacturonic acid-rich polysaccharides, was isolated through mild acid hydrolysis to degrade the linkages between neutral sugar side chains. Physico-chemical characterization was complemented by cryo-SEM micrographs indicating that RGI subdomains (which are highly branched) exhibited branch-like features, while the HG subdomains showed strand-like structures. This study provides an insight into the structure of carrot serum pectin and revealing the structural characteristics of serum pectin is an important step towards directing

structural changes to attain specific functionalities such as gelling, thickening or emulsifying. For more information, it might be interesting to explore the specific sugar linkages present.

Acknowledgements

We acknowledge the financial support of the Research Foundation Flanders (FWO grant G.0D17.14N) and the KU Leuven Research Council (METH/14/03) through its long term structural funding program—Methusalem funding by the Flemish Government. C. Kyomugasho is a postdoctoral fellow financially supported by Onderzoeksfonds KU Leuven Postdoctoral Fellowship (PDM). We would also like to thank the Hercules foundation for its financial support in acquiring the cryo-SEM (grant no. AUGE-09-029) used in this research. Finally, we thank Benny Lewille and Mohd Dona Bin Sintang from the Laboratory of Food Technology and Engineering, Department of Food Safety and Food Quality, Ghent University for all their valuable contributions in the use of the cryo-SEM.

References

Alba, K., Laws, A. P., & Kontogiorgos, V. (2015). Isolation and characterization of acetylated LM-pectins extracted from okra pods. Food Hydrocolloids, 43, 726-735.

Arnous, A., & Meyer, A. S. (2008). Comparison of methods for compositional characterization of grape (Vitis vinifera L.) and apple (Malus domestica) skins. *Food and Bioproducts Processing, 86*(2), 79-86.

Bonnin, E., Dolo, E., Le Goff, A., & Thibault, J. F. (2002). Characterisation of pectin subunits released by an optimised combination of enzymes.pdf>. *Carbohydrate Research, 337*, 1687-1696.

Caffall, K. H., & Mohnen, D. (2009). The structure, function, and biosynthesis of plant cell wall pectic polysaccharides. *Carbohydr Res, 344*(14), 1879-1900.

Christiaens, S., Van Buggenhout, S., Chaula, D., Moelants, K., David, C. C., Hofkens, J., Van Loey, A. M., & Hendrickx, M. E. (2012). In situ pectin engineering as a tool to tailor the consistency and syneresis of carrot purée. *Food Chemistry, 133*(1), 146-155.

Christiaens, S., Uwibambe, D., Uyttebroek, M., Van Droogenbroeck, B., Van Loey, A. M., & Hendrickx, M. E. (2015). Pectin characterisation in vegetable waste streams: A

starting point for waste valorisation in the food industry. LWT - Food Science and Technology, 61(2), 275-282.

De Ruiter, G. A., Schols, H. A., Voragen, A. G. J., & Rombouts, F. M. (1992). Carbohydrate analysis of water-soluble uronic acid-containing polysaccharides with high-performance anion-exchange chromatography using methanolysis combined with TFA hydrolysis is superior to four other methods. *Analytical Biochemistry, 207*(1), 176-185.

Endress, H. U., Mattes, F., & Norz, K. (2006). Pectins. In Y. H. Hui (Ed.), *Handbook of food science, technology and engineering* (pp. 140–1-140-35). CRC Taylor & Francis.

Houben, K., Christiaens, S., Ngouémazong, D. E., Van Buggenhout, S., Van Loey, A. M., & Hendrickx, M. E. (2014). The Effect of Endogenous Pectinases on the Consistency of Tomato–Carrot Purée Mixes. *Food and Bioprocess Technology, 7*(9), 2570-2580.

Houben, K., Jolie, R. P., Fraeye, I., Van Loey, A. M., & Hendrickx, M. E. (2011). Comparative study of the cell wall composition of broccoli, carrot, and tomato: structural characterization of the extractable pectins and hemicelluloses. *Carbohydr Res, 346*(9), 1105-1111.

Immerzeel, P., Eppink, M. M., de Vries, S. C., Schols, H. A., & Voragen, A. G. J. (2006). Carrot arabinogalactan proteins are interlinked with pectins. *Physiologia Plantarum, 128*(1), 18-28.

Ishii, T., Matsunaga, T., Pellerin, P., O'Neill, M. A., Darvill, A., & Albersheim, P. (1999). The Plant Cell Wall Polysaccharide Rhamnogalacturonan II Self-assembles into a Covalently Cross-linked Dimer. The American Society for Biochemistry and Molecular Biology, Inc, 274 (19)(May), 13098-13104.

Jamsazzadeh Kermani, Z., Shpigelman, A., Kyomugasho, C., Van Buggenhout, S., Ramezani, M., Van Loey, A. M., & Hendrickx, M. E. (2014). The impact of extraction with a chelating agent under acidic conditions on the cell wall polymers of mango peel. *Food Chem, 161*, 199-207.

Kaya, M., Sousa, A. G., Crepeau, M. J., Sorensen, S. O., & Ralet, M. C. (2014). Characterization of citrus pectin samples extracted under different conditions: influence of acid type and pH of extraction. *Ann Bot, 114*(6), 1319-1326.

Kravtchenko, T. P., Arnould, I., Voragen, A. G. J., & Pilnik, W. (1992). Improvement of the selective depolymerization of pectic substances by chemical β-elimination in aqueous solution. Carbohydr Polym, 237-242.

Kravtchenko, T. P., Voragen, A. G. J., & Pilnik, W. (1992). Analytical comparison of three industrial pectin preparations. Carbohydr Polymers, 18, 17-25.

Kravtchenko, T. P., Penci, M., Voragen, A. G. J., & Pilnik, W. (1993). Enzymic and chemical degradation of some industrial pectins. *Carbohydrate Polymers*, *20*(3), 195–205.

Kyomugasho, C., Christiaens, S., Shpigelman, A., Van Loey, A. M., & Hendrickx, M. E. (2015). FT-IR spectroscopy, a reliable method for routine analysis of the degree of methylesterification of pectin in different fruit- and vegetable-based matrices. *Food Chem, 176*, 82-90.

Kyomugasho, C., Christiaens, S., Van de Walle, D., Van Loey, A. M., Dewettinck, K., & Hendrickx, M. E. (2016). Evaluation of cation-facilitated pectin-gel properties: Cryo-SEM visualisation and rheological properties. *Food Hydrocolloids, 61*, 172-182.

Kyomugasho, C., Willemsen, K. L., Christiaens, S., Van Loey, A. M., & Hendrickx, M. E. (2015). Microscopic evidence for Ca(2+) mediated pectin-pectin interactions in carrot-based suspensions. *Food Chem, 188*, 126-136.

Massiot, P., Rouau, X., & Thibault, J. F. (1988). Characterisation of the extractable pectins and hemicelluloses of the cell wall of carrot. *Carbohydrate Research, 172*, 229-242.

Moelants, K. R. N., Cardinaels, R., Van Buggenhout, S., Van Loey, A. M., Moldenaers, P., & Hendrickx, M. E. (2014). A Review on the Relationships between Processing, Food Structure, and Rheological Properties of Plant-Tissue-Based Food Suspensions. *Comprehensive Reviews in Food Science and Food Safety, 13*(3), 241-260.

Moelants, K. R. N., Jolie, R. P., Palmers, S. K. J., Cardinaels, R., Christiaens, S., Van Buggenhout, S., Van Loey, A. M., Moldenaers, P., & Hendrickx, M. E. (2012). The Effects of Process-Induced Pectin Changes on the Viscosity of Carrot and Tomato Sera. *Food and Bioprocess Technology, 6*(10), 2870-2883.

Mohnen, D. (2008). Pectin structure and biosynthesis. *Curr Opin Plant Biol, 11*(3), 266-277.

Morris, G. A., Ralet, M.-C., Bonnin, E., Thibault, J.-F., & Harding, S. E. (2010). Physical characterisation of the rhamnogalacturonan and homogalacturonan fractions of sugar beet (Beta vulgaris) pectin. *Carbohydrate Polymers, 82*(4), 1161-1167.

Nagel, A., Sirisakulwat, S., Carle, R., & Neidhart, S. (2014). An acetate-hydroxide gradient for the quantitation of the neutral sugar and uronic acid profile of pectins by HPAEC-PAD without postcolumn pH adjustment. *J Agric Food Chem, 62*(9), 2037-2048.

O'Neill, M. A. O., Warrenfeltz, D., Kates, K., Pellerin, P., Doco, T., Darvill, A. G., & Albersheim, P. (1996). Rhamnogalacturonan-II, a Pectic Polysaccharide in the Walls of Growing Plant Cell, Forms a Dimer That Is Covalently Cross-linked by a Borate Ester. *The Journal of Biological Chemistry, 271 (37)*, 22923–22930.

Ridley, B. L., O'Neill, M. A., & Mohnen, D. (2001). Pectins: structure, biosynthesis, and oligogalacturonide-related signaling. *Phytochemistry, 57*, 929–967.

Round, A. N., Rigby, N. M., MacDougall, A. J., & Morris, V. J. (2010). A new view of pectin structure revealed by acid hydrolysis and atomic force microscopy. *Carbohydr Res, 345*(4), 487-497.

729 Santiago, J. S. J., Christiaens, S., Van Loey, A. M., & Hendrickx, M. E. (2016). Deliberate
730 processing of carrot purées entails tailored serum pectin structures. *Innovative Food*
731 *Science & Emerging Technologies, 33*, 515-523.
732
733 Santiago, J. S. J., Jamsazzadeh Kermani, Z., Xu, F., Van Loey, A. M., & Hendrickx, M. E.
734 (2017). The effect of high pressure homogenization and endogenous pectin-related
735 enzymes on tomato purée consistency and serum pectin structure. *Innovative Food*
736 *Science & Emerging Technologies, 43*, 35-44.
737
738 Sengkhamparn, N., Bakx, E. J., Verhoef, R., Schols, H. A., Sajjaanantakul, T., & Voragen, A.
739 G. (2009). Okra pectin contains an unusual substitution of its rhamnosyl residues with
740 acetyl and alpha-linked galactosyl groups. Carbohydr Res, 344(14), 1842-1851.
741
742 Shpigelman, A., Kyomugasho, C., Christiaens, S., Van Loey, A. M., & Hendrickx, M. E.
743 (2014). Thermal and high pressure high temperature processes result in distinctly
744 different pectin non-enzymatic conversions. *Food Hydrocolloids, 39*, 251-263.
745
746 Sila, D. N., Doungla, E., Smout, S., Van Loey, A. N., & Hendrickx, M. (2006). Pectin
747 Fraction Interconversions: Insight into Understanding Texture Evolution of Thermally
748 Processed Carrots. J. Agric. Food Chem., 54, 8471−8479

749 Sila, D. N., Van Buggenhout, S., Duvetter, T., Fraeye, I., De Roeck, A., Van Loey, A., &
750 Hendrickx, M. (2009). Pectins in Processed Fruits and Vegetables: Part II—
751 Structure– Function Relationships. *Comprehensive Reviews in Food Science and Food*
752 *Safety, 86-104*.

753 Thibault, J.-F., Renard, C. M. G. C., Axelos, M. A. V., Roger, P., & Crepeau, M.-J. (1993).
754 Studies of the length of homogalacturonic regions in pectins by acid hydrolysis.
755 *Carbohydrate Research, 238*, 271-286.
756
757 Voragen, F., Beldman,G., & Schols, H. (2001).Chemistry and enzymology of pectins. In B.
758 V. McCleary, & L. Prosky (Eds.), *Advanced dietary fiber technology* (pp. 379–398).
759 Oxford: Blackwell Science.
760
761 Voragen, A. G. J., Coenen, G.-J., Verhoef, R. P., & Schols, H. A. (2009). Pectin, a versatile
762 polysaccharide present in plant cell walls. *Structural Chemistry, 20*(2), 263-275.

763 Yapo, B. M., Lerouge, P., Thibault, J.-F., & Ralet, M.-C. (2007). Pectins from citrus peel cell
764 walls contain homogalacturonans homogenous with respect to molar mass,
765 rhamnogalacturonan I and rhamnogalacturonan II. Carbohydrate Polymers, 69(3),
766 426-435.

767
768

Figure captions:

Figure 1. Carrot purée preparation indicating the sequence of mechanical and thermal treatments with the respective sample codes (in italics). HT: high temperature treatment; HPH: high pressure homogenization; LT: low temperature treatment.

Figure 2. Size exclusion elution profiles of the RGI-rich fractions and alcohol insoluble residues (AIR) of the lyophilized serum obtained from differently-prepared carrot purées (A) log molar mass distribution (thick lines) superimposed on concentration chromatogram (thin curves) (B) Light scattering signal at 92° angle (thick curves) superimposed on UV absorbance chromatogram at 280 nm (thin curves). Solid lines for HT+HPH, long dash for HPH+HT and square dot lines for HPH+LT+HT sample. All grey colored lines represent de-esterified AIRs, while black colors for HG-rich fractions.

Figure 3. Size exclusion elution profiles of the HG-rich fractions and the respective de- de-esterified AIR of the (lyophilized) serum obtained from differently-prepared carrot purées (A) log molar mass distribution (thick lines) superimposed on concentration chromatogram (thin curves) (B) Light scattering signal at 92° angle (thick curves) superimposed on UV absorbance chromatogram at 280 nm (thin curves). Solid lines for HT+HPH, long dash for HPH+HT and square dot lines for HPH+LT+HT sample. All grey colored lines represent de-esterified AIRs, while black colors for HG-rich fractions.

Figure 4. Representative cryo-SEM images of carrot serum pectic polysaccharides with the respective RGI-rich and HG-rich fractions. Scale bars =1µm

Tables:

Table 1. Average monosaccharide composition (± SD) of the alcohol insoluble residues (AIRs) of lyophilized serum from differently-prepared carrot purées and isolated rhamnogalacturonan I-rich fractions (RGI). Different capital letters (in superscript) indicate statistical differences (p-value <0.05) among AIRs or RGI-rich fractions, while small letters indicate statistical difference between AIR and RGI-rich fraction. The values in parentheses indicate the mol % of each sugar. (HT: high temperature treatment at 95 °C for 30 min; HPH: high pressure homogenization at 100 MPa; LT: low temperature treatment at 60 °C for 40 min).

Sample codes		Monosaccharides (mg/g AIR)										
		Fuc	Rha	Ara	Gal	Gluc	Xyl	Man	GalA	GlucA	Total sugars	Total amount of pectin-associated sugars
HT+HPH	AIR	1.8 ± 0.2 ^{Aa} (0.3)	39.3 ± 0.9 ^{Aa} (6.0)	60.4 ± 3.7 ^{Aa} (10.5)	77.5 ± 10.2 ^{Aa} (11.6)	30.5 ± 6.7 ^{Aa} (5.1)	2.2 ± 0.8 ^{Aa} (0.5)	8.5 ± 1.7 ^{Aa} (1.3)	455.2 ± 71.9 ^{Aa} (63.9)	4.43 ± 3.63 ^{Aa} (0.8)	679.05 ± 100.57	636.5 ± 87.8
	RGI	1.2 ± 0.1 ^{Aa} (0.6)	26.6 ± 1.6 ^{Aa} (12.3)	43.4 ± 1.4 ^{Ab} (22.0)	62.4 ± 1.4 ^{Ab} (26.3)	4.4 ± 0.3 ^{Ab} (1.9)	1.4 ± 0.2 ^{ABa} (0.7)	2.4 ± 0.1 ^{Ab} (1.0)	97.4 ± 10.6 ^{Ab} (38.1)	3.28 ± 0.69 ^{Aa} (1.3)	242.69 ± 16.59	232.6 ± 15.4
HPH+HT	AIR	1.5 ± 0.1 ^{Aa} (0.3)	26.3 ± 0.7 ^{Ba} (4.5)	51.4 ± 0.4 ^{Aa} (9.6)	75.2 ± 2.8 ^{Aa} (11.7)	69.4 ± 0.0 ^{Ba} (10.8)	1.9 ± 0.2 ^{Aa} (0.4)	9.9 ± 0.6 ^{Aa} (1.5)	416.4 ± 12.5 ^{Aa} (60.1)	8.36 ± 0.82 ^{Aa} (1.2)	660.25 ± 18.17	572.6 ± 16.8
	RGI	0.9 ± 0.1 ^{Aa} (0.5)	16.7 ± 1.3 ^{Bb} (9.2)	35.7 ± 2.3 ^{Bb} (21.5)	56.1 ± 3.5 ^{Ab} (28.2)	5.7 ± 1.4 ^{Ab} (2.9)	1.1 ± 0.2 ^{Aa} (0.7)	2.4 ± 0.0 ^{Ab} (1.2)	75.4 ± 4.1 ^{ABb} (35.2)	1.47 ± 1.76 ^{Ab} (0.7)	195.53 ± 14.66	185.9 ± 11.5
HPH+LT+HT	AIR	1.7 ± 0.1 ^{Aa} (0.3)	19.6 ± 1.1 ^{Ca} (3.1)	66.2 ± 5.6 ^{Aa} (11.5)	117.6 ± 10.2 ^{Ba} (16.9)	66.9 ± 8.6 ^{Ba} (10.3)	4.0 ± 1.6 ^{Aa} (0.7)	16.8 ± 1.8 ^{Ba} (2.4)	358.4 ± 38.5 ^{Aa} (53.6)	7.88 ± 0.35 ^{Aa} (1.2)	659.08 ± 67.74	567.6 ± 57.1
	RGI	1.0 ± 0.0 ^{Aa} (0.5)	12.0 ± 1.2 ^{Bb} (5.8)	43.9 ± 0.6 ^{Ab} (23.3)	84.3 ± 0.0 ^{Bb} (37.3)	7.1 ± 2.0 ^{Ab} (3.1)	1.84 ± 0.04 ^{Ba} (1.0)	4.9 ± 0.6 ^{Bb} (2.2)	65.3 ± 0.3 ^{Bb} (26.8)	0.25 ± 0.23 ^{Ab} (0.1)	220.64 ± 5.00	208.3 ± 2.2

Table 2a. Average pectin-related sugar ratios, DM and protein content (± SD) of the rhamnogalacturonan I-rich fractions (RGI) and their respective alcohol insoluble residues (AIR) obtained from the lyophilized serum of differently-prepared carrot purées. Different capital letters (in superscript) indicate statistical differences (p-value <0.05) among AIRs or RGI-rich fractions, while small letters indicate statistical difference between AIR and RGI-rich fraction. (HT: high temperature treatment at 95 °C for 30 min; HPH: high pressure homogenization at 100 MPa; LT: low temperature treatment at 60 °C for 40 min).

Sample codes		Linearity of pectin (GalA/Fuc+Rha+Ara+Gal+Xyl)	Contribution of RGI (Rha/GalA)	Branching of RGI (Ara+Gal/Rha)	Protein (% d.b.)	DM (%)
HT+HPH	AIR	2.2 ± 0.1^{ABa}	0.09 ± 0.01^{Aa}	3.7 ± 0.1^{Aa}	9.6 ± 0.04^{Aa}	65.3 ± 0.5^{Aa}
	RGI	0.6 ± 0.1^{Ab}	0.32 ± 0.02^{Ab}	3.9 ± 0.1^{Aa}	1.8 ± 0.08^{Ab}	4.4 ± 0.7^{Ab}
HPH+HT	AIR	2.3 ± 0.1^{Aa}	0.07 ± 0.01^{Ba}	4.8 ± 0.2^{Ba}	7.2 ± 0.01^{Ba}	65.1 ± 1.1^{Aa}
	RGI	0.6 ± 0.1^{Ab}	0.26 ± 0.01^{ABb}	5.4 ± 0.4^{Aa}	1.2 ± 0.03^{Ab}	4.6 ± 1.1^{Ab}
HPH+LT+HT	AIR	1.7 ± 0.2^{Ba}	0.06 ± 0.01^{Ca}	9.1 ± 0.3^{Ca}	13.4 ± 0.01^{Aa}	52.1 ± 1.7^{Ba}
	RGI	0.4 ± 0.1^{Bb}	0.22 ± 0.02^{Bb}	10.5 ± 1.1^{Ba}	3.2 ± 0.09^{Bb}	5.6 ± 0.3^{Ab}

Table 2b. Average molecular weight, intrinsic viscosity and mass fraction (± SD) for each corresponding polymer population of alcohol insoluble residue (AIR) and its rhamnogalacturonan I-rich fraction. Different capital letters (in superscript) indicate statistical differences (p-value <0.05) among AIRs or RGI-rich fractions, while small letters indicate statistical difference between AIR and RGI-rich fraction. (HT: high temperature treatment at 95 °C for 30 min; HPH: high pressure homogenization at 100 MPa; LT: low temperature treatment at 60 °C for 40 min).

Sample codes		M_w (kDa)		Intrinsic viscosity (dl/g)		Fraction of mass found	
		Population I	Population II	Population I	Population II	Population I	Population II
HT+HPH	AIR	1370.0 ± 42.4^{Aa}	130.0 ± 8.5^{Aa}	2.30 ± 0.03^{Aa}	1.14 ± 0.03^{Aa}	0.19 ± 0.02^{Aa}	0.41 ± 0.02^{Aa}
	RGI	98.5 ± 00.3^{Ab}	10.4 ± 0.4^{Ab}	0.37 ± 0.01^{Ab}	0.08 ± 0.01^{Ab}	0.29 ± 0.01^{Ab}	0.34 ± 0.02^{Aa}
HPH+HT	AIR	577.5 ± 33.2^{Ba}	57.1 ± 1.8^{Ba}	2.22 ± 0.05^{Aa}	0.94 ± 0.02^{Ba}	0.09 ± 0.01^{Ba}	0.53 ± 0.01^{Ba}
	RGI	119.5 ± 00.7^{Bb}	14.8 ± 0.1^{Bb}	0.37 ± 0.01^{Bb}	0.09 ± 0.01^{Ab}	0.24 ± 0.01^{Bb}	0.41 ± 0.02^{Bb}
HPH+LT+HT	AIR	132.5 ± 06.4^{Ca}	15.8 ± 2.6^{Ca}	1.42 ± 0.03^{Ba}	0.09 ± 0.01^{Ca}	0.46 ± 0.01^{Ca}	0.13 ± 0.01^{Ca}
	RGI	119.0 ± 01.4^{Bb}	15.4 ± 0.9^{Ba}	0.25 ± 0.01^{Cb}	0.08 ± 0.01^{Aa}	0.19 ± 0.01^{Cb}	0.45 ± 0.01^{Bb}

Table 3. Average monosaccharide composition (± SD) of the homogalacturonan-rich fractions (HG) and de-esterified alcohol insoluble residues (de-AIR) of lyophilized serum obtained from differently-prepared carrot purées. Different capital letters (in superscript) indicate statistical differences (*p*-value <0.05) among de-esterified AIRs or HG-rich fractions, while small letters indicate statistical difference between de-esterified AIR and HG-rich fraction. The values in parentheses indicate the mol % of each sugar. (HT: high temperature treatment at 95 °C for 30 min; HPH: high pressure homogenization at 100 MPa; LT: low temperature treatment at 60 °C for 40 min).

Sample codes		Monosaccharides (mg/g de-esterified AIR)										
		Fuc	Rha	Ara	Gal	Gluc	Xyl	Man	GalA	GlucA	Total sugars	Total amount of pectin-associated sugars
HT+HPH	De-esterified AIR	1.9 ± 0.1 ^{Aa} (0.3)	36.8 ± 0.6 ^{Aa} (6.5)	57.1 ± 2.1 ^{ABa} (11.1)	75.3 ± 2.0 ^{Aa} (12.2)	11.7 ± 2.9 ^{Aa} (1.9)	3.7 ± 0.0 ^{Aa} (0.7)	6.0 ± 1.8 ^{Aa} (1.0)	436.9 ± 34.9 ^{Aa} (65.6)	4.7 ± 0.9 ^{Aa} (0.7)	634.2 ± 45.33	611.7 ± 39.6
	HG	0.1 ± 0.0 ^{Ab} (0.0)	11.2 ± 0.3 ^{Ab} (3.3)	1.3 ± 1.2 ^{Ab} (0.4)	8.0 ± 0.3 ^{Ab} (2.2)	6.4 ± 2.3 ^{Aa} (1.7)	3.5 ± 2.8 ^{Aa} (1.1)	4.0 ± 2.0 ^{Aa} (1.1)	354.1 ± 29.5 ^{Aa} (89.7)	1.44 ± 0.3 ^{Ab} (0.4)	389.9 ± 38.6	378.1 ± 34.1
HPH+HT	De-esterified AIR	1.5 ± 0.3 ^{Aa} (0.3)	27.6 ± 1.8 ^{Ba} (5.1)	51.8 ± 4.7 ^{Ba} (10.6)	73.2 ± 10.0 ^{Aa} (12.4)	13.4 ± 5.7 ^{Aa} (2.3)	2.2 ± 0.5 ^{Aa} (0.4)	7.9 ± 2.5 ^{Aa} (1.3)	425.4 ± 42.8 ^{Aa} (67.1)	2.9 ± 1.0 ^{Aa} (0.4)	605.9 ± 71.1	581.7 ± 60.0
	HG	0.0 ± 0.0 ^{Ab} (0.0)	7.5 ± 0.6 ^{Bb} (2.3)	0.7 ± 0.5 ^{Ab} (0.2)	10.0 ± 0.6 ^{Ab} (2.8)	4.8 ± 0.2 ^{Aa} (1.4)	1.1 ± 0.0 ^{Aa} (0.4)	2.2 ± 1.4 ^{Aa} (0.6)	352.6 ± 13.0 ^{Aa} (92.0)	1.4 ± 0.2 ^{Aa} (0.4)	380.3 ± 16.4	371.9 ± 14.7
HPH+LT+HT	De-esterified AIR	1.6 ± 0.0 ^{Aa} (0.3)	20.8 ± 0.2 ^{Ca} (3.8)	67.3 ± 0.2 ^{Aa} (13.3)	121.6 ± 3.6 ^{Ba} (20.0)	10.7 ± 0.3 ^{Aa} (1.8)	2.3 ± 0.5 ^{Aa} (0.4)	9.4 ± 1.7 ^{Aa} (1.5)	377.8 ± 31.2 ^{Aa} (57.8)	6.7 ± 1.4 ^{Aa} (1.0)	618.0 ± 39.2	591.3 ± 35.7
	HG	0.0 ± 0.0 ^{Ab} (0.0)	5.3 ± 0.4 ^{Cb} (1.7)	0.2 ± 0.0 ^{Ab} (0.1)	19.6 ± 3.4 ^{Bb} (5.6)	5.0 ± 0.3 ^{Ab} (1.4)	1.8 ± 0.2 ^{Aa} (0.6)	2.3 ± 0.0 ^{Ab} (0.7)	335.7 ± 39.6 ^{Aa} (89.4)	1.8 ± 0.6 ^{Ab} (0.5)	371.8 ± 44.5	362.8 ± 43.6

Table 4a. Average pectin-related sugar ratios, DM and protein content (± SD) of homogalacturonan-rich fractions compared to the de-esterified alcohol insoluble residues (de-esterified AIR) obtained from the lyophilized serum of differently-prepared carrot purées. Different capital letters (in superscript) indicate statistical differences (p-value <0.05) among de-esterified AIRs or HG-rich fractions, while small letters indicate statistical difference between de-esterified AIR and HG-rich fraction. (HT: high temperature treatment at 95 °C for 30 min; HPH: high pressure homogenization at 100 MPa; LT: low temperature treatment at 60 °C for 40 min).

Sample codes		Linearity of pectin (GalA/Fuc+Rha+Ara+Gal+Xyl)	Branching of RGI (Ara+Gal/Rha)	Contribution of RGI (Rha/GalA)	Protein (% d.b.)	DM (%)
HT+HPH	De-esterified AIR	2.1 ± 0.1 ^{Aa}	3.6 ± 0.1 ^{Aa}	0.10 ± 0.01 ^{Aa}	7.4 ± 0.1 ^{Aa}	8.6 ± 1.0 ^{Aa}
	HG	12.6 ± 0.1 ^{Ab}	0.8 ± 0.1 ^{Ab}	0.04 ± 0. 01 ^{Ab}	3.1 ± 0.1 ^{Ab}	8.0 ± 0.3 ^{Aa}
HPH+HT	De-esterified AIR	2.3 ± 0.1 ^{Aa}	4.5 ± 0.2 ^{Ba}	0.08 ± 0.01 ^{Ba}	4.9 ± 0.2 ^{Ba}	7.0 ± 1.0 ^{ABa}
	HG	16.1 ± 0.1 ^{Bb}	1.3 ± 0.2 ^{Ab}	0.03 ± 0.01 ^{ABb}	1.5 ± 0.1 ^{Bb}	6.0 ± 0.3 ^{Ba}
HPH+LT+HT	De-esterified AIR	1.5 ± 0.1 ^{Ba}	8.9 ± 0.2 ^{Ca}	0.07 ± 0.01 ^{Ba}	8.2 ± 0.1 ^{Aa}	5.9 ± 0.7 ^{Ba}
	HG	11.1 ± 1.2 ^{Cb}	3.4 ± 0.8 ^{Bb}	0.02 ± 0.01 ^{Bb}	3.3 ± 0.1 ^{Ab}	5.7 ± 0.7 ^{Ba}

Table 4b. Average molecular weight, intrinsic viscosity and mass fraction (± SD) for each corresponding polymer population of de-esterified alcohol insoluble residue (de-esterified AIR) and derived homogalacturonan-rich fractions (HG). Different capital letters (in superscript) indicate statistical differences (p-value <0.05) among de-esterified AIRs or HG-rich fractions, while small letters indicate statistical difference between de-esterified AIR and HG-rich fraction. (HT: high temperature treatment at 95 °C for 30 min; HPH: high pressure homogenization at 100 MPa; LT: low temperature treatment at 60 °C for 40 min).

Sample codes		M_w (kDa)		Intrinsic viscosity (dl/g)		Fraction of mass found	
		Population I	Population II	Population I	Population II	Population I	Population II
HT+HPH	De-esterified AIR	534.0 ± 125 ^{Aa}	61.8 ± 12.5 ^{Aa}	0.84 ± 0.10 ^{Aa}	0.57 ± 0.11 ^{Aa}	0.09 ± 0.02 ^{Aa}	0.51 ± 0.10 ^{Aa}
	HG	222.0 ± 9.2 ^{Ab}	17.2 ± 0.1 ^{Ab}	1.39 ± 0.03 ^{Ab}	0.44 ± 0.01 ^{Ab}	0.05 ± 0.01 ^{Aa}	0.55 ± 0.01 ^{Aa}
HPH+HT	De-esterified AIR	513.0 ± 18.4 ^{Aa}	63.4 ± 1.7 ^{Aa}	0.94 ± 0.07 ^{Aa}	0.61 ± 0.02 ^{Aa}	0.05 ± 0.01 ^{Aa}	0.60 ± 0.04 ^{Aa}
	HG	219.5 ± 2.1 ^{Ab}	23.4 ± 8.1 ^{Ab}	1.79 ± 0.01 ^{Ab}	0.46 ± 0.02 ^{Ab}	0.03 ± 0.01 ^{Aa}	0.57 ± 0.04 ^{Aa}
HPH+LT+HT	De-esterified AIR	148.5 ± 4.9 ^{Ba}	32.1 ± 2.9 ^{Ba}	0.67 ± 0.10 ^{Ba}	0.46 ± 0.01 ^{Ba}	0.24 ± 0.02 ^{Ba}	0.46 ± 0.11 ^{Aa}
	HG	32.6 ± 0.2 ^{Bb}	13.2 ± 1.2 ^{Bb}	0.78 ± 0.03 ^{Ba}	0.34 ± 0.01 ^{Bb}	0.25 ± 0.01 ^{Ba}	0.31 ± 0.06 ^{Ba}

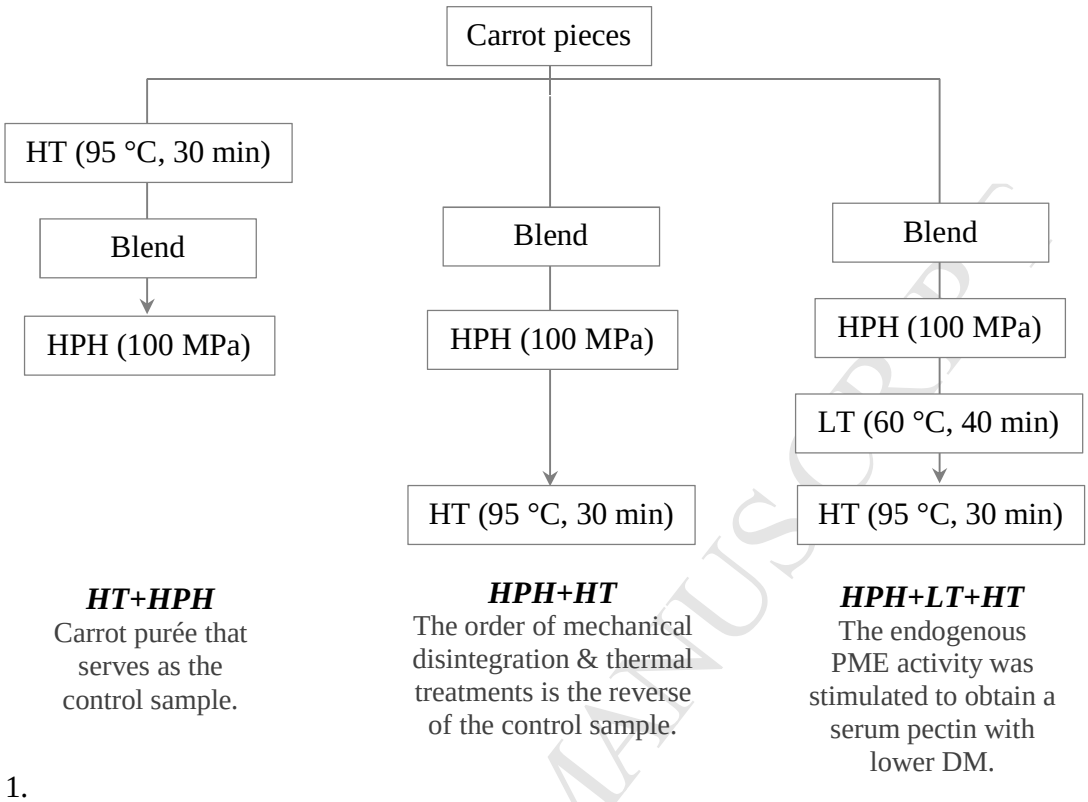

Figure 1.

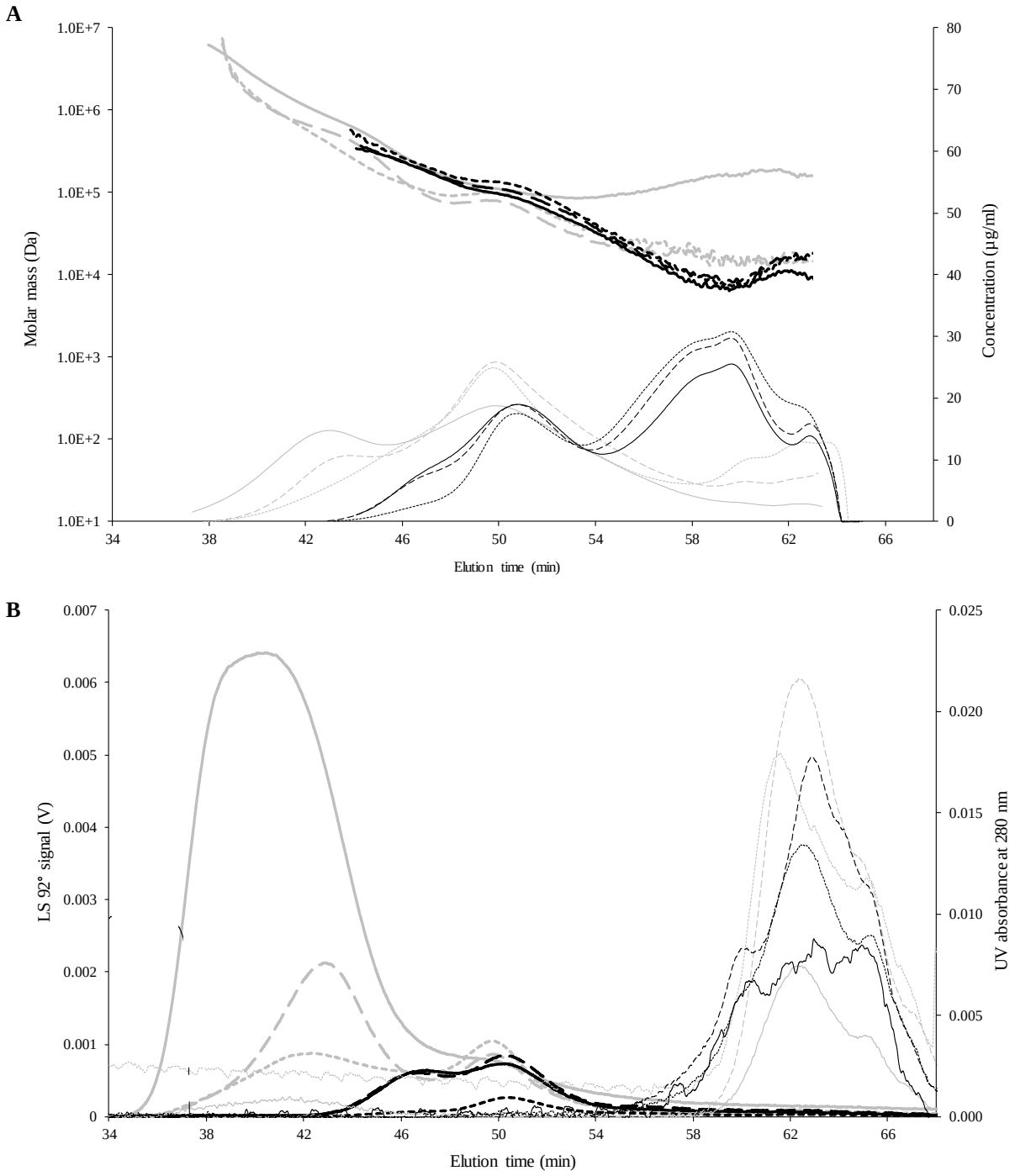
A
Molar mass (Da)
Concentration (µg/ml)
Elution time (min)
B
LS 92° signal (V)
UV absorbance at 280 nm
Elution time (min)

Figure 2.

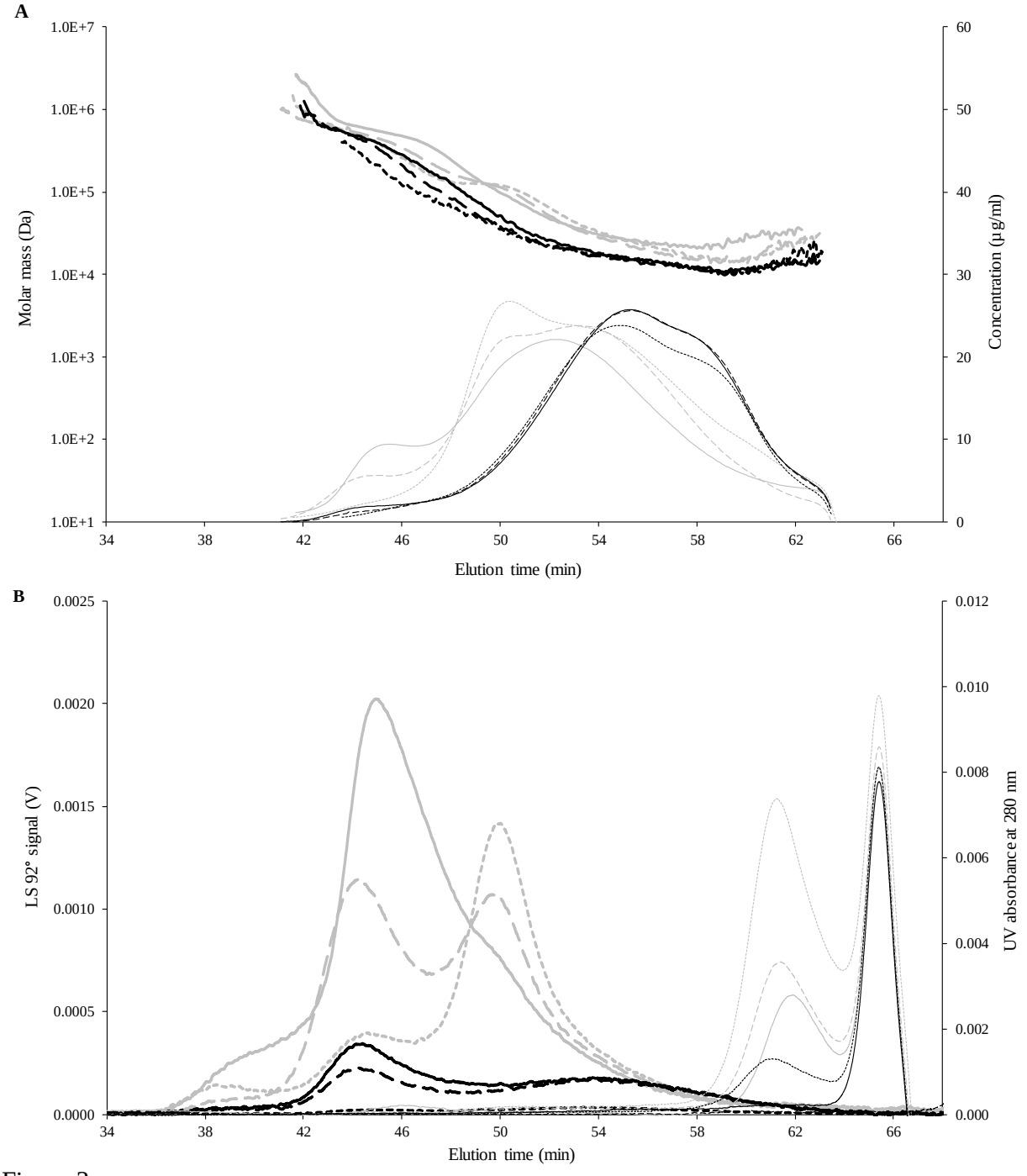
A
1.0E+7
1.0E+6
1.0E+5
1.0E+4
1.0E+3
1.0E+2
1.0E+1
Molar mass (Da)
60
50
40
30
20
10
0
Concentration (µg/ml)
34
38
42
46
50
54
58
62
66
Elution time (min)
B
0.0025
0.0020
0.0015
0.0010
0.0005
0.0000
LS 92° signal (V)
0.012
0.010
0.008
0.006
0.004
0.002
0.000
UV absorbance at 280 nm
34
38
42
46
50
54
58
62
66
Elution time (min)

Figure 3.

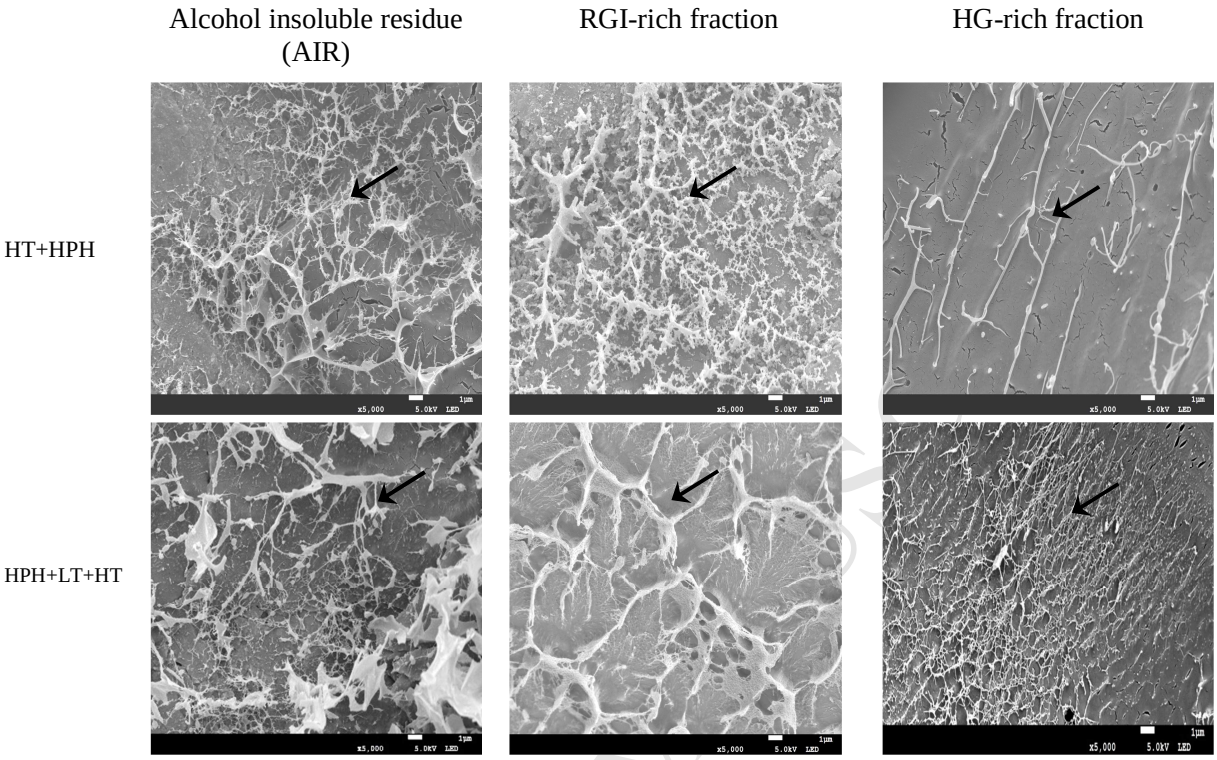

Figure 4.